Visible detection of performance controlling pinholes in silica encapsulation films

Fiona M Elam[1-3], Yaoge Liu[1,2], Bernadette C A M van der Velden-Schuermans[3], Sergey A Starostin[3], Mauritius C M van de Sanden[1,2] and Hindrik W de Vries[1]
[1]DIFFER – Dutch Institute for Fundamental Energy Research, P.O. Box 6336, 5600 HH Eindhoven, The Netherlands.
[2]Eindhoven University of Technology, Applied Physics, P.O. Box 513, 5600 MB Eindhoven, The Netherlands.
[3]FUJIFILM Manufacturing Europe B.V., P.O. Box 90156, 5000 LJ Tilburg, The Netherlands.

E-mail: m.c.m.vandesanden@differ.nl

Abstract. For the first time in atmospheric pressure-plasma enhanced chemical vapour deposition of amorphous silica onto flexible polymer substrates, pinholes have been visibly detected using interferometric microscopy and their average diameter of 1.7 μm calculated. Pinholes were found to control the water vapour transmission rate of all 30 nm films deposited with input energies greater than 9 keV per precursor molecule, thus presenting an opportunity for the synthesis of single layer thin films with precisely targeted permeation rates. The pinholes themselves were understood to originate from interactions between the polymer substrate and filaments in the plasma. The non-uniformity of the discharge was attributed to the reduced concentrations of precursor tetraethyl orthosilicate and oxygen species necessary to deposit amorphous silica at high specific energies.

1. Introduction

Roll-to-roll atmospheric pressure-plasma enhanced chemical vapour deposition (AP-PECVD) is an innovative technology that can be integrated into many existing manufacturing systems to facilitate the cost effective mass production of functional films; specifically encapsulation foils [1,2]. These barrier films are essential to the flexible electronics industry, envisioned to protect devices such as flexible photovoltaics, thin film transistors, quantum dot liquid crystal displays and organic light emitting diodes against degradation from oxygen and water [3].

AP-PECVD, like many other deposition methods, has certain limitations. The most prominent is the creation of pinholes in the deposited films under ‘harsh processing conditions’, namely long plasma residence times in conjunction with low precursor flux [4]. These processing conditions are thought to induce specific plasma-surface interactions such as substrate etching [5–8], which can in turn result in the formation of pinholes. In a recent study [4], it was found that pinhole formation could be prevented in silica films deposited upon a polymer substrate using AP-PECVD, if a bilayer film structure was applied. A low density silica layer was deposited directly onto the substrate under lenient conditions, prior to the deposition of the dense, active silica barrier layer, and thus acted as a protective coating to prevent plasma-surface interactions [4].

Unsurprisingly, pinholes have been detected and studied in silica films deposited using a variety of techniques [9–15], but to our knowledge have not been examined to a great extent in films deposited on

polymer substrates (namely polyethylene 2,6 naphthalate, PEN) using AP-PECVD. The focus of the presented work is to attempt to detect these pinholes visibly, determine their size, and to evaluate their influence upon the encapsulation performance of intrinsically dense single layer silica barrier films. Increasing our understanding of the nature and occurrence of these performance limiting pinholes can present potential opportunities to tune the porosity of single layer silica thin films for specific applications, based upon the deposition conditions of this industrially and commercially relevant manufacturing method.

2. Experimental

A roll-to-roll glow-like AP dielectric barrier discharge (DBD) open to ambient air was used to synthesise 30 nm (27 ± 4 nm) silica-like single layer films by PECVD. The set-up is located in an ISO class 3 cleanroom, in accordance with ISO 14644-1 standards. A schematic representation of the AP-PECVD reactor can be found in [1], illustrating two cylindrical rotary drum electrodes (with radii 120 mm; and 0.5 mm gaseous gap) connected to a matching network, power supply, a voltage probe (Passive High Voltage Probe P6015A, Tektronix) and current probe (Pearson current monitor model 4100, Pearson Electronics, Inc.). The electrodes were heated to 80 ± 1 °C, and the temperature of the polymer substrate (dielectric material) that covered each electrode, was monitored using an infrared camera (FLIR A320, FLIR Systems Co Ltd.).

The plasma (ignited between the two drum electrodes) was created using a high frequency generator (L3001, Seren Industrial Power Systems), tuned within the range 180–200 kHz in order to optimise forward power matching. The PECVD reactor was operated in the pulsed mode, with pulse lengths of 800 μs and a 90% duty cycle. The voltage amplitude measured between the two drum electrodes was 2–3 kV. The power dissipated in the discharge was 600 W, with a reflected power in the range 2–5% of the forward signal, and thus corresponded to a specific power density of approximately 0.2 W mm^{-2} (assuming an effective plasma discharge width of 150 mm, and a 20 mm expansion along the gas flow). The peak current density averaged over the treated surface area was estimated to reach 1.7 mA mm^{-2}. The I-V waveforms of the discharge during deposition can be found in a publication by Starostin et al. [1]. In order to monitor the uniformity of the plasma throughout the deposition process, a sensitive array camera (Eclipse EC-11-05h40, DALSA) with a 13 μs frame integration time was utilised.

Polyethylene 2,6 naphthalate (PEN) foil (Teonex Q65HA, Teijin DuPont Films) with a width and depth of 180 mm and 100 μm respectively, was used as the substrate material and positioned over the lower drum electrode. To enable the deposition of a ~30 nm silica layer, the foil transport speed was varied from 372–35 mm min^{-1}. Polyethylene terephthalate (PET) (ASTERATM Functional Foils, AGFA), was used as the dielectric material for the upper drum electrode, and the transport speed maintained at 50 mm min^{-1} in all cases.

Reactant gases in all instances were oxygen (technical grade) and tetraethyl orthosilicate ($Si(OC_2H_5)_4$, TEOS) (≥99.0%, Sigma-Aldrich). The precursor gas, TEOS, was injected via a controlled evaporation mixer unit (CEM-Technology, Bronkhorst HIGH-TECH B.V.), where the vapours were combined with 1 slm argon (technical grade). Nitrogen (technical grade) with a flow of 20 slm, was used as the carrier gas. All four gases were combined in the gas injector before being released into the plasma. The TEOS and oxygen gas flows were adjusted with a fixed ratio of 4.5×10^{-3} in the range of 3.6×10^{-3}–0.2×10^{-3} slm and 0.8–0.05 slm respectively, in order to vary the input energy per TEOS molecule and therefore the layer densities [1,2]. This resulted in the deposition of silica layers with input energies ranging from approximately 3–30 keV/TEOS molecule. Equation 1 [1], related to the Yasuda composite power parameter [16], was used to calculate the input energy per TEOS molecule for each silica layer,

$$Energy\ per\ TEOS\ molecule = \frac{P_d}{R_{dep}\rho} \cdot \frac{M}{N_A} \quad (1)$$

where P_d is the power density in the discharge, R_{dep} is the deposition rate of silica layers simultaneously upon two substrate webs [1], (also expressed as $\frac{dh}{dt_{dep}}$, where h and t_{dep} are film thickness and deposition

time respectively), ρ is the density of amorphous silica (2.2 g cm^{-3}), M is the molar mass of silica (SiO_2) and N_A is Avogadro's Number. The Yasuda composite power parameter was originally used to determine input energies for plasma polymerisation [16]. However, Equation 1 is based upon elements that relate directly to the deposited amorphous silica layer [1], rather than upon the flow rate and molecular weight of the precursor molecule. For the studied conditions, the reactor was operating in the complete precursor depletion mode. It should also be noted that because of system limitations, for films deposited with oxygen gas flows below 0.075 slm, dry air was used as the reactant gas in place of oxygen.

To determine the exact thickness of the silica layers post-deposition, spectroscopic ellipsometry was performed using a variable angle spectroscopic ellipsometer (M-2000D, J.A. Woollam Co. Inc.). Operational parameters are listed in recent publications by Starostin et al. and Elam et al. [1,2].

Regarding pinhole detection, two approaches were utilised. The primary method employed interferometric microscopy (IM) (Wyko NT9100 Optical Profiling System, Veeco Instruments Inc.) of the pristine silica surface, analysing areas of 47×63 μm^2 in phase-shift interferometry mode with an optical resolution of 0.49 μm. A series of 10 individual images were processed, resulting in the overall evaluation of 0.03 mm^2 for every sample. Pinholes visibly deeper than 6 nm and greater than 1μm in diameter were recorded. The secondary method involved exposure of the films to a solvent with a molecular kinetic diameter of 0.33 nm, thus small enough to permeate through pinholes in the silica [17], to the PEN substrate and induce blister formation at the location of each pinhole. IM in vertical scanning mode was then performed post-exposure, in order to detect for the presence of the blisters and hence pinholes in the silica layers [4]. Areas of 47×63 μm^2 were analysed and resulting micrographs processed and stitched to form images with areas of 25 mm^2 using Wyko Vision software. The pinhole density (pinhole number per cm^2) was calculated from an average of 10 stitched interferometric micrographs, with circular peaks greater than 0.3 μm in height considered pinholes. In total, an area of 2.5 cm^2 was evaluated for every sample.

In order to determine the influence of the pinholes upon the encapsulating performance of the films comprising the 30 nm silica layer and PEN substrate, a Deltaperm (Technolox Ltd.), with set conditions of 40 °C, 90% relative humidity (RH) was used to establish the effective water vapour transmission rate (WVTR) of each sample. A detailed description of the method can be found in [2].

3. Results and discussion

A representative interferometric microscopy (IM) image of the pristine surface of a 30 nm silica layer deposited with an input energy of 6.0 keV per tetraethyl orthosilicate (TEOS) precursor molecule, can be seen in Figure 1, alongside a corresponding IM image that illustrates the outcome of the solvent vapour exposure analysis performed on the same sample. For the first time in the reported surface analysis of amorphous silica films deposited on polymer substrates using AP-PECVD, pinholes (represented by the ~1 μm diameter blue circles in Figure 1a) are distinctly visible in an interferometric micrograph. Previous studies [4], have so far failed to provide direct visual evidence for their existence, despite using techniques such as atomic force microscopy (AFM) to analyse the morphology of the amorphous silica surface. This is however, largely due to the relatively low pinhole density with respect to the AFM scanning areas applied (2×2 μm^2), and consequently reduces the probability of detection [4].

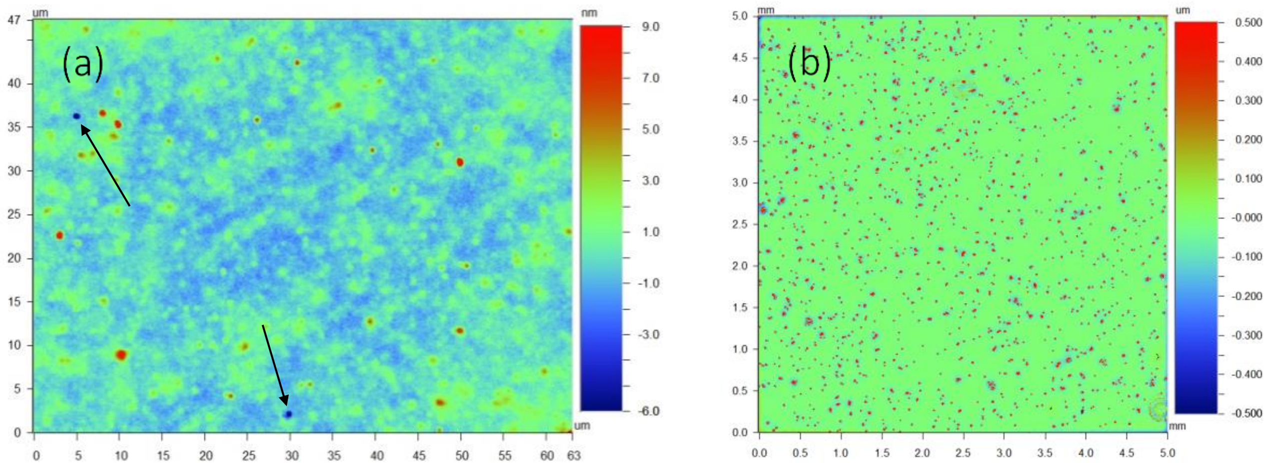

Figure 1. Interferometric micrographs of a 30 nm silica encapsulation film deposited with an input energy of 6.0 keV/TEOS molecule illustrating: (a) the pristine silica surface revealing two ~1 µm diameter pinholes (blue circles) indicated by arrows and (b) the typical outcome of solvent vapour exposure analysis, with small high features indicative of blister formation resulting primarily from the presence of pinholes [4].

The density of the pinholes in the IM images found via the direct analysis of the pristine surface and by the solvent vapour exposure method was quantified, and plotted as a function of increasing input energy per TEOS molecule during the deposition process. A graphical representation is shown in Figure 2.

There is a distinct disparity between the two detection methods regarding the magnitude of error in the pinhole density data obtained. This is most likely due to the difference in the sample area analysed for each technique. An area of 250 mm^2 was evaluated per sample using the solvent vapour exposure method, whereas for the IM images of the pristine silica surface, only 0.03 mm^2 per sample was examined. The solvent vapour exposure technique is therefore considerably more statistically reliable. Also noticeable in Figure 2 is the large discrepancy between the pinhole densities determined by the two methods for the sample deposited at the lowest input energy. This probably results from the accidental inclusion of non-penetrating pinholes during the analysis of the IM images of the pristine surface, thus accounting for the increased pinhole density reported.

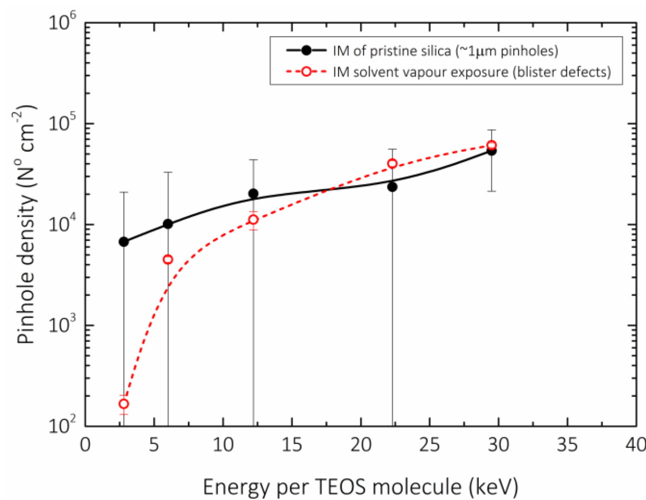

Figure 2. Pinhole density data obtained from IM analysis of the pristine silica surface and solvent vapour exposure analysis plotted as a function of increasing input energy per TEOS molecule during the deposition process [4].

In order to establish if there was in fact a significant difference between the two methods used to determine the pinhole density, a two-tailed Mann-Whitney U Test was performed with a 5% level of significance ($\alpha = 0.05$). The null and two-tailed research hypotheses for the nonparametric test are stated as follows:

H_0: The two populations are equal
H_1: The two populations are not equal

If the observed value of U is less than or equal to the critical value, H_0 is rejected in favour of H_1, and if the observed value of U exceeds the critical value, H_0 is not rejected. For a two-tailed level of significance ($\alpha = 0.05$) and sample size $n_1 = n_2 = 5$, $U_{crit} = 2$. In the investigated case, $U_{obs} = 11$, thus H_0 is not rejected as $11 > 2$. Therefore, there is no statistically significant evidence at $\alpha = 0.05$, to show that the pinhole density data obtained via solvent vapour exposure analysis, and the density data acquired from the detection of ~1 μm diameter pinholes in pristine silica layers, are not equal. Based upon this finding, it can be concluded that the size distribution of the pinholes found in the silica layers is likely to be relatively uniform.

In order to ascertain the impact of the supposedly 1 μm diameter pinholes upon the encapsulating performance of the 30 nm silica films deposited using AP-PECVD, the effective water vapour transmission rate (WVTR) of each film was measured. A plot of the effective WVTR Q, of each sample as a function of the number of pinholes per square centimetre n, (detected using the statistically more reliable solvent vapour exposure technique) is shown in Figure 3. It is quite clear that for films deposited at input energies greater than approximately 6 keV/TEOS molecule, the effective WVTR is not regulated by the intrinsic film porosity [2,4], but controlled by the pinholes. This observation is emphasised by the strongly positive linear correlation (Pearson's correlation coefficient, $r = 1$), defined by the straight line with equation $Q = 0.0931n - 0.0185$ (and associated slope and intercept errors of 0.4% and 8.1% respectively), which essentially intersects the origin and also assumes a uniform pinhole diameter. Consequently, it should be possible, based purely upon the pinhole density, to estimate the WVTR of any 30 nm single layer silica film with a pinhole density greater than ~11000 pinholes cm^{-2}.

Moreover, from the inserted graph in Figure 3, the specific input energy per TEOS molecule E, at which the effective WVTR Q, becomes pinhole controlled for 30 nm silica layers can be identified. A perfect linear association (Pearson's correlation coefficient, $r = 1$), is observed between the WVTR and input energy per TEOS molecule of films deposited with energies greater than 12.2 keV. Hence extrapolation of this line with equation $Q = 0.0268E - 0.242$ (and respective slope and intercept errors of 0.6% and 1.4%) to $Q = 0$, reveals an input energy threshold of 9.03 keV per TEOS molecule, after which the effective WVTR becomes theoretically pinhole controlled. Therefore, provided the input energy per TEOS molecule is greater than ~9 keV, the effective WVTR of a 30 nm single layer silica film can potentially be targeted, determined by the specific input energy during the AP-PECVD process.

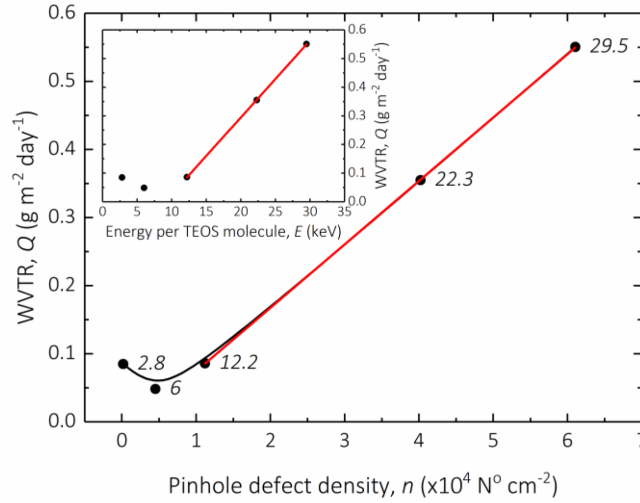

Figure 3. Effective WVTR (at 40 °C, 90%RH) plotted as a function of increasing pinhole density (with labels corresponding to input energy (keV) per TEOS molecule during the deposition process). The inserted graph illustrates how the effective WVTR changes with input energy per TEOS molecule.

As the effective WVTR of the 30 nm silica films deposited at energies greater than ~9 keV/TEOS molecule is clearly governed by pinholes, it is possible to calculate their average diameter and thus validate the visibly detected pinhole size. Equation 2, obtained from a publication by Da Silva Sobrinho, et al. [18], describes permeation through encapsulation barrier coatings containing numerous pinholes with uniform radius R_0:

$$Q = \frac{Nq_p}{At} = n\left(2\pi R_0 D\Phi_0 + \frac{\pi R_0^2 D\Phi_0}{L_p}\right) \tag{2}$$

where Q is the transmission rate through the whole sample of surface area A, $n = N/A$ is the number density of pinholes, q_p quantity of permeant leaving the polymer substrate in time t, D is the diffusion coefficient of the polymer substrate, Φ_0 is the partial pressure of the permeant in the gas phase if it does not interact with the polymer substrate, and L_p is the thickness of the polymer substrate. Equation 2 can be simplified by substitution of Equation 3, which describes the transmission rate through the polymer substrate Q_p, to give Equation 4:

$$Q_p = \frac{q_p}{At} = \frac{D\Phi_0}{L_p} \tag{3}$$

$$Q = n\left(2\pi R_0 Q_p L_p + \pi R_0^2 Q_p\right) \tag{4}$$

The average pinhole radius R_0 can then be calculated by substituting Equation 4 into the straight line equation from Figure 3 that demonstrates the relation between water vapour transmission rate Q and pinhole density n, to give Equation 5:

$$Q = 0.0931n\left(\pi R_0 Q_p\left(2L_p + R_0\right)\right) - 0.0185 \tag{5}$$

By solving the differential of Equation 5 for R_0, thus gives an average pinhole radius of 0.878 ± 0.003 µm, and hence average diameter 1.76 ± 0.01 µm. The calculated and observed values are therefore in agreement, confirming that ~1 µm diameter pinholes directly control the effective WVTR of 30 nm single layer silica films deposited at specific energies greater than ~9 keV/TEOS molecule. The calculated and observed values are also within the range of diameters reported by Deilmann et al. (0.25–

3.09 μm) for pinholes in 60 nm silica coatings deposited onto polyethylene terephthalate using a low-pressure microwave plasma reactor [12]; and close to the upper range of diameters determined using conductive atomic force microscopy by Marathe et al. (0.1–1.3 μm) for ~3 nm silica grown by thermal oxidation onto p-type silicon [9].

Regarding the origin of the ~1 μm pinholes, gradually intensified processing conditions (sustained plasma and heat exposure in conjunction with decreased precursor availability) required to deposit films at specific energies greater than 6 keV/TEOS molecule, induce plasma-polymer interactions such as etching [5–8], that are thought to result in said pinhole formation [4]. The polymer substrate is exposed to a one order of magnitude increase in energy per unit area from 5.8×10^{5} to 6.8×10^{6} J m^{-2}, between depositions carried out at the lowest and highest specific energies, due to the necessary reduction in foil transport speed through the plasma. However, other processes may also influence the existence of pinholes.

The uniformity of the plasma throughout the deposition process is monitored using a sensitive array camera (Eclipse EC-11-05h40, DALSA) with a 13 μs frame integration time. It displays the time evolution of the discharge light emission in a vertical direction, with the dark horizontal bands corresponding to the plasma 'off' intervals for the 90% duty cycle. During deposition conditions necessary to generate silica layers at increased specific energies, the output of the array camera revealed a reduction in discharge uniformity, suggesting that the plasma was no-longer completely glow-like, but became partially filamentary across the width of the discharge, evident from the increasing presence of vertical lines (Figure 4a–c). Based upon this observation, additional images were taken of the discharge emission using a digital camera (OM-D E-M10 Mark II, Olympus) with 4 ms exposure time to illustrate the nature of the filamentation at the boundary of the discharge (Figure 4d–f). Due to system limitations, a replica DBD was used to obtain the digital camera images [19], but operated under otherwise comparable conditions, utilizing a 200 kHz low frequency power source to excite the discharge. It is therefore possible, that under conditions of reduced precursor and oxygen concentration [20], and in the absence of a protective coating for the polymer substrate [4], enhanced filamentation can arise and trigger the formation of pinholes in the deposited silica layers, via interaction with the substrate material. These plasma-polymer interactions would be particularly enhanced near the boundaries of the discharge, where the bare substrate is directly exposed to the plasma.

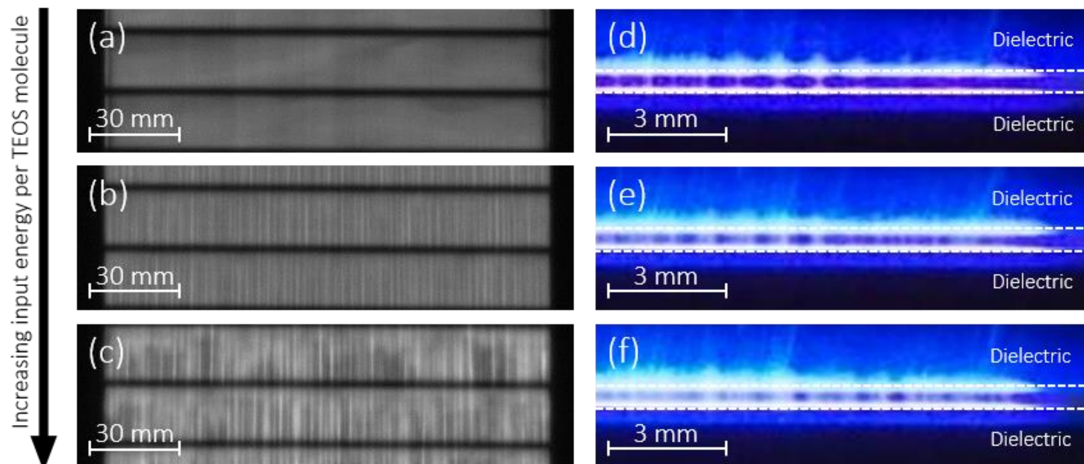

Figure 4. The nature of the plasma discharge during the deposition process under conditions similar to those used for the generation of the 30 nm silica layers. All images depict the front-view of the plasma discharge: (a)–(c) representative array camera images with a 13 μs frame integration time showing gradually enhanced filamentation across the entire width of the 150 mm discharge as a function of increasing input energy per TEOS molecule (decreasing TEOS and oxygen concentrations) and (d)–(f) equivalent digital camera images with 4 ms exposure times illustrating enhanced filamentation at the right side edge of the discharge boundary. Dotted lines indicate the position of the dielectric layers above and below the discharge. Some of the emission may be due to reflection.

4. Conclusions

In conclusion, pinholes in 30 nm amorphous silica thin films deposited onto a PEN substrate using roll-to-roll AP-PECVD were visibly detected for the first time using low magnification interferometric imaging. Both the observed and calculated average pinhole diameters (~1 μm) were in agreement, and within the range reported in literature. The size distribution of the pinholes was also relatively uniform. The effective WVTR of films deposited at specific energies greater than ~9 keV/TEOS molecule was found to be pinhole controlled. This therefore presents an opportunity for the synthesis of single layer films with precisely targeted permeation rates, determined by the specific input energy per TEOS molecule during the AP-PECVD process. The pinholes themselves were understood to originate from the interaction of the polymer substrate with filaments in the plasma discharge. It is highly likely that the reduced concentrations of precursor and oxygen necessary to deposit silica layers at high specific energies, attributed to the non-uniformity of the discharge.

Acknowledgements

This research received funding from the European Union's Seventh Framework Programme for research, technological development and demonstration under grant agreement number 606889; project ESR7 in the framework of the RAPID (Reactive Atmospheric Plasma processIng – eDucation network) Marie Curie Initial Training Network (www.rapid-itn.eu). The work is also in association with the Industrial Partnership Programme i31 (APPFF) that is carried out under an agreement between FUJIFILM Manufacturing Europe B.V. and FOM, which is part of the Netherlands Organisation for Scientific Research (NWO). The author would like to thank R. van Beijnen, E. Gommers and B. Korngold (FUJIFILM Manufacturing Europe B.V., Tilburg, The Netherlands) for their technical assistance.

References

[1] Starostin S A, Creatore M, Bouwstra J B, van de Sanden M C M and de Vries H W 2015 Towards roll-to-roll deposition of high quality moisture barrier films on polymers by atmospheric pressure plasma assisted process *Plasma Process. Polym.* **12** 545–54

[2] Elam F M, Starostin S A, Meshkova A S, van der Velden-Schuermans B C A M, Bouwstra J B, van de Sanden M C M and de Vries H W 2017 Atmospheric pressure roll-to-roll plasma enhanced CVD of high quality silica-like bilayer encapsulation films *Plasma Process. Polym.* **14** 1600143

[3] Lewis J 2006 Material challenge for flexible organic devices *Mater. Today* **9** 38–45

[4] Elam F M, Starostin S A, Meshkova A S, van der Velden-Schuermans B C A M, van de Sanden M C M and de Vries H W 2017 Defect prevention in silica thin films synthesised using AP-PECVD for flexible electronic encapsulation *J. Phys. D. Appl. Phys.* **50** 25LT01

[5] Fang Z, Wang X, Shao R, Qiu Y and Edmund K 2011 The effect of discharge power density on polyethylene terephthalate film surface modification by dielectric barrier discharge in atmospheric air *J. Electrostat.* **69** 60–6

[6] Zhang C, Shao T, Long K, Yu Y, Wang J, Zhang D, Yan P and Zhou Y 2010 Surface treatment of polyethylene terephthalate films using DBD excited by repetitive unipolar nanosecond pulses in air at atmospheric pressure *IEEE Trans. Plasma Sci.* **38** 1517–26

[7] Fang Z, Yang H and Qiu Y 2010 Surface treatment of polyethylene terephthalate films using a microsecond pulse homogeneous dielectric barrier discharges in atmospheric air *IEEE Trans. Plasma Sci.* **38** 1615–23

[8] Liu Y, Welzel S, Starostin S A, van de Sanden M C M, Engeln R and de Vries H W 2017 Infrared gas phase study on plasma-polymer interactions in high-current diffuse dielectric

barrier discharge *J. Appl. Phys.* **121** 243301

[9] Marathe V G, Stefanov Y, Schwalke U and Dasgupta N 2006 Study of pinholes in ultrathin SiO2 by C-AFM technique *Thin Solid Films* **504** 11–4

[10] Nagata H, Fujino T, Mitsugi N and Tamai M 1998 Effect of substrate heating on elimination of pinholes in sputtering deposited SiO2 films on LiNbO3 single crystal substrates *Thin Solid Films* **335** 117–21

[11] da Silva Sobrinho A S, Czeremuszkin G, Latrèche M, Dennler G and Wertheimer M R 1999 A study of defects in ultra-thin transparent coatings on polymers *Surf. Coatings Technol.* **116–119** 1204–10

[12] Deilmann M, Halfmann H, Steves S, Bibinov N and Awakowicz P 2009 Silicon oxide permeation barrier coating and plasma sterilization of PET bottles and foils *Plasma Process. Polym.* **6** 695–9

[13] Macech P and Pemberton J E 2009 Passivation of pinhole defect microelectrode arrays in ultrathin silica films immobilized on gold substrates *Thin Solid Films* **517** 5399–403

[14] Dameron A, Davidson S D, Burton B, Carcia P F, McLean R S and George S M 2008 Gas diffusion barriers on polymers using multilayers fabricated by Al2O3 and rapid SiO2 atomic layer deposition *J. Phys. Chem. C* **112** 4573–80

[15] Perrotta A, García S J, Michels J, Andringa A-M and Creatore M 2015 Analysis of nanoporosity in moisture permeation barrier layers by electrochemical impedance spectroscopy *ACS Appl. Mater. Interfaces* **7** 15968–77

[16] Yasuda H K 1985 *Plasma Polymerization* (Orlando, FL, USA: Academic Press Inc.)

[17] Roberts A P, Henry B M, Sutton A P, Grovenor C R M, Briggs G A D, Miyamoto T, Kano M, Tsukahara Y and Yanaka M 2002 Gas permeation in silicon-oxide/polymer (SiOx/PET) barrier films: Role of the oxide lattice, nano-defects and macro-defects *J. Memb. Sci.* **208** 75–88

[18] da Silva Sobrinho A S, Czeremuszkin G, Latrèche M and Wertheimer M R 2000 Defect-permeation correlation for ultrathin transparent barrier coatings on polymers *J. Vac. Sci. Technol. A Vacuum, Surfaces, Film.* **18** 149–57

[19] Liu Y, Peeters F J J, Starostin S A, van de Sanden M C M and de Vries H W 2018 Improving uniformity of atmospheric-pressure dielectric barrier discharges using dual frequency excitation *Plasma Sources Sci. Technol.* **27** 01LT01

[20] Wormeester G, Pancheshnyi S, Luque A, Nijdam S and Ebert U 2010 Probing photo-ionization: simulations of positive streamers in varying N2 : O2-mixtures *J. Phys. D. Appl. Phys.* **43** 505201